Deletion of microRNA-155 reduces autoantibody responses and alleviates lupus-like disease in the *Fas*^{lpr} mouse

To-Ha Thai[a,1], Heide Christine Patterson[b,c,d,e,2], Duc-Hung Pham[a,f,2], Katalin Kis-Toth[a], Denise A. Kaminski[g], and George C. Tsokos[a]

[a]Department of Medicine, Beth Israel Deaconess Medical Center, Harvard Medical School, Boston, MA 02115; [b]Whitehead Institute for Biomedical Research, Cambridge, MA 02142; [c]Department of Pathology, Brigham and Women's Hospital, Boston, MA 02115; [d]Laboratory for Molecular Medicine, Partners HealthCare Center for Personalized Genetic Medicine, Cambridge, MA 02139; [e]Institut fuer Klinische Chemie und Biochemie, Klinikum rechts der Isar, 81675 München, Germany; [f]Department of Pharmacokinetics, Toxicology and Targeting, University of Groningen, 9713 AV, Groningen, The Netherlands; and [g]College Writing Program, University of Rochester, Rochester, NY 14627

Edited by Max D. Cooper, Emory University, Atlanta, GA, and approved November 4, 2013 (received for review September 21, 2013)

MicroRNA-155 (miR-155) regulates antibody responses and subsequent B-cell effector functions to exogenous antigens. However, the role of miR-155 in systemic autoimmunity is not known. Using the death receptor deficient (*Fas*^{lpr}) lupus-prone mouse, we show here that ablation of miR-155 reduced autoantibody responses accompanied by a decrease in serum IgG but not IgM anti-dsDNA antibodies and a reduction of kidney inflammation. MiR-155 deletion in *Fas*^{lpr} B cells restored the reduced SH2 domain-containing inositol 5′-phosphatase 1 to normal levels. In addition, coaggregation of the Fc γ receptor IIB with the B-cell receptor in miR-155$^{-/-}$-*Fas*^{lpr} B cells resulted in decreased ERK activation, proliferation, and production of switched antibodies compared with miR-155 sufficient *Fas*^{lpr} B cells. Thus, by controlling the levels of SH2 domain-containing inositol 5′-phosphatase 1, miR-155 in part maintains an activation threshold that allows B cells to respond to antigens.

ERK pathways | SHIP-1

MicroRNA-155 (miR-155) plays a critical role in the generation of effective antibody responses to exogenous antigenic challenges in mice (1–3). MiR-155 levels have been reported to be elevated in B but low in T cells from patients with systemic lupus erythamosus (4), yet it is not known whether miR-155 controls autoimmune responses and the expression of related pathology.

Mice harboring ubiquitous or B-cell-specific ablation of the death receptor Fas develop a severe lupus-like disease. B-cell-specific deletion of the death receptor (*fas*$^{-/-}$) *fas*$^{-/-}$ mice develop an excessive germinal center (GC)-derived IgG autoantibody deposition in their kidneys and succumb to renal failure (5). It has been suggested that loss of tolerance in *lpr* mice results from the down-regulation of the low-affinity IgG inhibitory receptor FcγRIIB (Fc γ receptor IIB), thereby rendering their B cells incapable of terminating stimulatory signals delivered by autoantigen-containing immune complexes (6–8). However, the mechanisms whereby lack of FcγRIIB engagement would lead to autoimmunity, and whether additional factors contribute to autoimmunity, are still unclear.

The SH2 domain-containing inositol 5′-phosphatase 1 (SHIP-1) phosphatase acts downstream of inhibitory cell-surface receptors (9–12), including the FcγRIIB, which is essential in opposing B-cell activation signals in mice and humans (13, 14). FcγRIIB inactivation has been implicated in the development of autoreactive GC B cells and plasma cells (15), as well as in the regulation of the persistence and longevity of bone marrow plasma cells (16). After coligation of the FcγRIIB with the B-cell receptor (BCR), FcγRIIB recruits SHIP-1 to the plasma membrane, where it negatively regulates cell survival, Ca^{2+}-dependent effector functions, and ERK activation, thus controlling cell proliferation, anergy, and apoptosis (17–23). As a consequence of these wide-ranging activities, germ-line or B-cell-specific deletion of FcγRIIB or SHIP-1 in mice results in a severe lupus-like disease characterized by high-titer serum IgG antinuclear autoantibodies, lymphadenopathy, splenomegaly, renal failure, and increased mortality (23–27). MiR-155 has been reported to regulate SHIP-1 expression in mammalian myeloid and malignant B cells (28–31). However, it is not known whether SHIP-1 regulation by miR-155 affects GC reactions or peripheral tolerance during a protective immune response or in an autoimmune environment, such as that in *Fas*^{lpr} mice.

To understand the role of miR-155 in autoimmunity, we crossed *Fas*^{lpr} mice with our *bic*/miR-155$^{-/-}$ mice to generate miR-155$^{-/-}$-*Fas*^{lpr} animals. Here we demonstrate that deletion of miR-155 reduced serum IgG but not IgM anti-dsDNA autoantibody levels and kidney damage. Further, we show that the absence of miR-155 derepresses the expression of SHIP-1, thus mitigating B-cell activation, proliferation, and autoimmune responses. We provide evidence that miR-155 could be targeted to control autoimmunity and lupus nephritis.

Results

Ablation of miR-155 Mitigates Splenomegaly in the *Fas*^{lpr} Mouse. B-cell-specific or ubiquitous inactivation of Fas leads to early death preceded by a lymphoproliferative disorder manifested as splenomegaly and lymphadenopathy (5, 32). Compared with the aged-matched *Fas*^{lpr} group (mean size: 0.432 ± 0.01 g), miR-155$^{-/-}$-*Fas*^{lpr} mice had a 2.8-fold reduction in their spleen size

Significance

The host immune system provides diverse defense mechanisms to fight harmful bacteria and viruses. One of these mechanisms is the production of antibodies targeting infectious agents. However, the production of antibodies has to be tightly controlled. Insufficient control of the immune system may result in the development of autoimmune diseases, including lupus. Lupus is characterized by the production of antibodies attacking the kidneys, leading to life-threatening kidney failure if untreated. In this study, we show that microRNA-155, one member of a family of regulatory molecules, promotes the production of antibodies. By deleting microRNA-155, we can prevent the production of harmful antibodies and alleviate lupus-like disease in mice. Our results suggest the possibility of targeting microRNA-155 to treat autoimmune diseases.

Author contributions: T.-H.T. designed research; H.C.P., D.-H.P., and K.K.-T. performed research; T.-H.T., D.-H.P., D.A.K., and G.C.T. analyzed data; and T.-H.T., D.-H.P., and D.A.K. wrote the paper.

The authors declare no conflict of interest.

This article is a PNAS Direct Submission.

[1]To whom correspondence should be addressed. E-mail: tthai@bidmc.harvard.edu.

[2]H.C.P. and D.-H.P. contributed equally to this work.

This article contains supporting information online at www.pnas.org/lookup/suppl/doi:10.1073/pnas.1317632110/-/DCSupplemental.

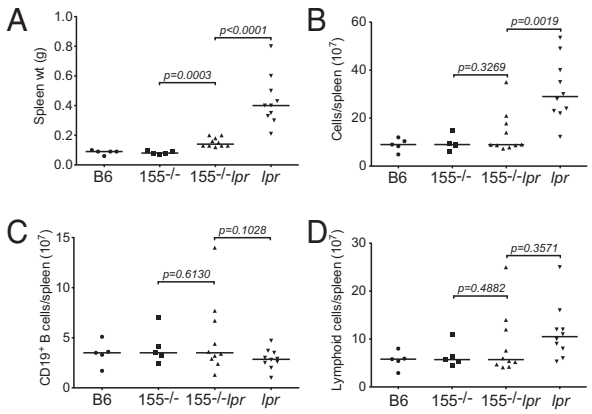

Fig. 1. Ablation of miR-155 alleviates splenomegaly in the *Fas*^{lpr} mouse. Results were obtained from aged mice (10-12 mo old). WT B6 (n = 5); miR-155$^{-/-}$ (n = 5); miR-155$^{-/-}$-*Fas*^{lpr} (n = 10); *Fas*^{lpr} (n = 10). (*A*) Spleens were weighed before analysis. Each symbol represents one mouse. (*B*) The number of live spleen cells was determined by Trypan blue. (*C*) The number of lymphoid cells per spleen was calculated from the number of live cells within the lymphoid gate. (*D*) The number of CD19^{+} spleen B cells was calculated from the lymphoid population. *P* values were determined by Student *t* test (GraphPad Software).

(mean size: 0.153 ± 0.05 g, $P < 0.0001$, Fig. 1*A* and Fig. S1). The smaller spleen size of miR-155$^{-/-}$-*Fas*^{lpr} mice was accompanied by a 2.3-fold lower total number of cells in this tissue compared with the *Fas*^{lpr} mice (mean 1.4×10^8 vs. 3.2×10^8, $P = 0.0019$, Fig. 1*B*). There was a consistent normalization of total lymphoid and CD19^{+} B cells in the miR-155$^{-/-}$-*Fas*^{lpr} spleen (Fig. 1 *C* and *D*). Additionally, miR-155$^{-/-}$-*Fas*^{lpr} mice had smaller peripheral lymph nodes (pLNs); however, the degree of reduction in their size varied considerably. We did not observe a change in the frequency of the unusual peripheral CD4^{-}CD8^{-} T cells in miR-155$^{-/-}$-*Fas*^{lpr} mice compared with *Fas*^{lpr} mice (Fig. S2) (32). Overall, these data show that targeting of miR-155 limits the development of splenomegaly and lymphadenopathy in *Fas*^{lpr} mice.

Autoantigen-Induced GC Reactions Are Reduced in miR-155$^{-/-}$-*Fas*^{lpr} Mice. Spontaneous GC reactions observed in *Fas*^{lpr} mice have been demonstrated to be autoantigen-driven (33, 34). We and others have previously shown that GC reactions and subsequent B-cell effector functions are regulated by miR-155 (1–3). We thus asked whether miR-155 deletion would mitigate spontaneous GC reactions in *fas*-deficient mice. Flow cytometry confirmed that compared with the age-matched B6 parental strain, 10- to 12-mo-old *Fas*^{lpr} mice had a higher frequency of B cells with the GC phenotype, peanut agglutinin (PNA)$^{+}$GL7^{+} (Fig. 2*A*). However, the frequency of GC-phenotype B cells in miR-155$^{-/-}$-*Fas*^{lpr} spleens (1.75% ± 0.65%) and pLNs (0.76% ± 0.29%) was fivefold and 12-fold lower, respectively, compared with *Fas*^{lpr} mice (spleen GC B cells 8.82% ± 0.4%, $P < 0.0001$; pLN GC B cells 9.0% ± 0.9%, $P = 0.0013$, Fig. 2 *A*–*C*). The lower GC B-cell frequency corresponded to a statistically significant reduction in the total number of spleen GC B cells in miR-155$^{-/-}$-*Fas*^{lpr} mice (Fig. 2*D*). Thus, in miR-155$^{-/-}$-*Fas*^{lpr} mice, both the frequency and total number of spleen and the frequency of pLN GC B cells were normalized to the levels seen in B6 and miR-155$^{-/-}$ control mice. At the time of analysis, aged (10–12 mo old) *Fas*^{lpr} mice developed severe lymphadenopathy with many large pLNs, possibly generated from the fusion of many nodes, making it difficult to confidently ascertain that the absolute number of GC B cells observed were representative of individual pLNs. Histologically, PNA staining of follicular structures confirmed spontaneous GC formation in *Fas*^{lpr} lymphoid tissues (Fig. 2*E*). By contrast, miR-155$^{-/-}$-*Fas*^{lpr} spleens and pLNs contained a minimal number of GCs, comparable to

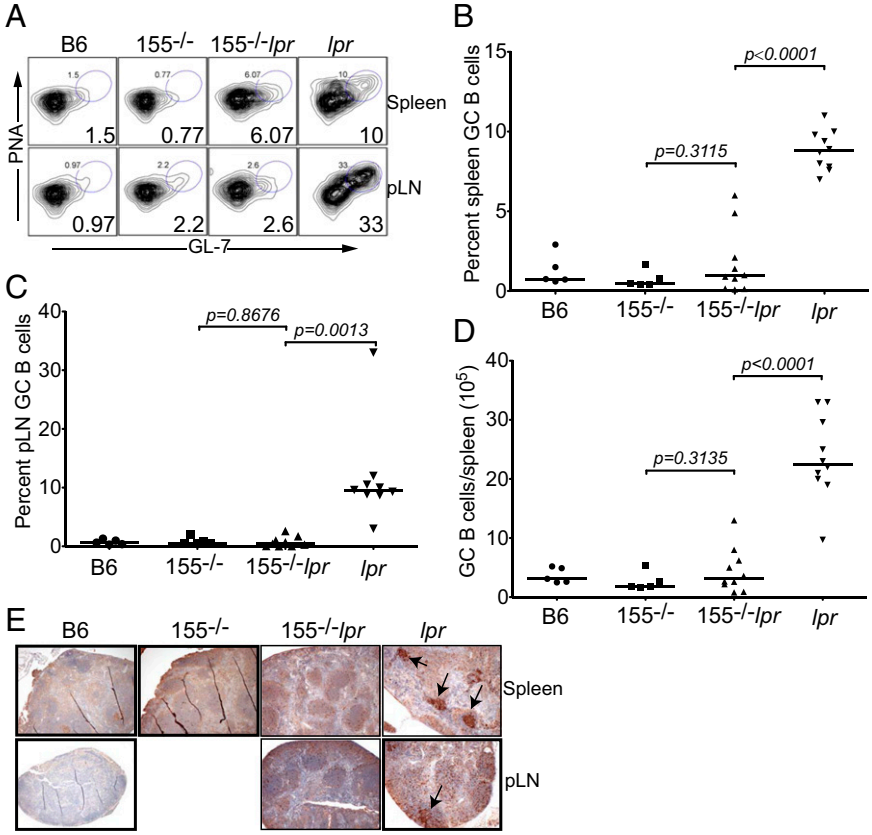

Fig. 2. Autoantigen-induced GC reactions are reduced in miR-155$^{-/-}$-*Fas*^{lpr} mice. (*A*) The frequency of GC B cells within the CD19 gate using PNA-phycoerythrin (PE) and GL-7-FITC. Plots are representative of 5–10 experiments. B6 (n = 5), miR-155$^{-/-}$ (n = 5), miR-155$^{-/-}$-*Fas*^{lpr} (n = 10), *Fas*^{lpr} (n = 10). (*B*) The frequency of spleen GC B cells within the CD19 gate was determined from *A*. Each symbol represents one mouse. (*C*) The frequency of pLN GC B cells within the CD19 gate was determined from *A*. (*D*) The absolute number of spleen GC B cells was calculated from *B*. *P* values were determined using the GraphPad Software Student *t* test. (*E*) Immunohistochemistry of spleens and pLNs was done using paraffin sections. Arrows indicates germinal centers stained with PNA (brown) and counterstained with hematoxylin. Blue stain indicates follicles.

those in B6 and miR-155$^{-/-}$ control mice (Fig. 2*E*, arrows indicate GCs). Therefore, in addition to controlling GC formation in response to exogenous antigens (1), miR-155 participates in autoantigen-driven GC reactions in the *Fas*^{lpr} mouse.

Serum IgG Anti-dsDNA Autoantibodies Are Decreased in miR-155$^{-/-}$-*Fas*^{lpr} Mice. A marker of human systemic lupus erythamosus is the presence of high-titer IgG autoantibodies against nuclear autoantigens, especially dsDNA (35, 36). Similarly, aged *Fas*^{lpr} or B-cell-specific *fas*-deficient mice produce excessive amounts of autoantibodies directed against dsDNA or ssDNA autoantigens (5, 32). As early as 8 wk of age and before the onset of overt kidney pathology, total serum IgM and IgG anti-dsDNA autoantibodies were high in *Fas*^{lpr} mice compared with B6 controls, as expected (Fig. 3 *A* and *B*). By contrast, miR-155$^{-/-}$-*Fas*^{lpr} mice had ∼twofold lower levels of total IgG anti-dsDNA autoantibodies at all ages examined (Fig. 3*B*, $*P \leq 0.02$). However, miR-155$^{-/-}$-*Fas*^{lpr} mice maintained the same levels of IgM anti-dsDNA antibodies as in *Fas*^{lpr} mice (Fig. 3*A*). To understand the reason for the reduced serum IgG observed in miR-155$^{-/-}$-*Fas*^{lpr} mice, we carried out in vitro switched assays. B-cell cultures from B6, miR-155$^{-/-}$, and miR-155$^{-/-}$-*Fas*^{lpr} mice showed similar frequencies of IgG$_1$-positive (∼15%) and divided cells (∼33%) after stimulation (Fig. 3 *C*–*E*). By contrast, we observed a higher frequency of class-switched cells in the *Fas*^{lpr} cultures (29%), which corresponded to a higher frequency of divided cells (69%, Fig. 3 *C*–*E*). Overall, there was an ∼twofold decrease in the level of serum IgG anti-dsDNA and a 1.9-fold decrease in switched IgG$_1$ antibodies in miR-155$^{-/-}$-*Fas*^{lpr} compared with *Fas*^{lpr} mice. Therefore, miR-155 deficiency in part reduces B-cell proliferation and isotype-switched antibody production in *fas*-deficient *lpr* mice.

It has been suggested that most isotype-switched and somatically mutated autoantibodies produced in aged *lpr* mice originate from short-lived plasmablasts (B220^{+}, CD138^{+}, CD22^{low}) that develop outside the GC (37–39). However, in the *lpr* autoimmune environment, miR-155 deficiency did not change the frequency or number of B220^{+}CD138^{+}CD22^{low} B cells (Fig. S3 *A* and *B*). Our data suggest that in the *lpr* autoimmune environment, miR-155 controls the homeostasis of switched autoreactive B cells.

MiR-155 Deficiency Alleviates Lupus Nephritis in *fas*-Deficient Lupus-Prone Mice. *Fas*^{lpr} and B-cell-specific *fas*-deficient mice often succumb to renal failure associated with the overproduction of autoantibodies and immune-complex deposition in the kidneys (5, 32). We thus asked whether systemic B-cell changes in our miR155-deficient *lpr* mice correlated with changes in Igs deposition in their kidneys. Immunofluorescence staining revealed less IgG staining in the glomeruli of miR-155$^{-/-}$-*Fas*^{lpr} mice

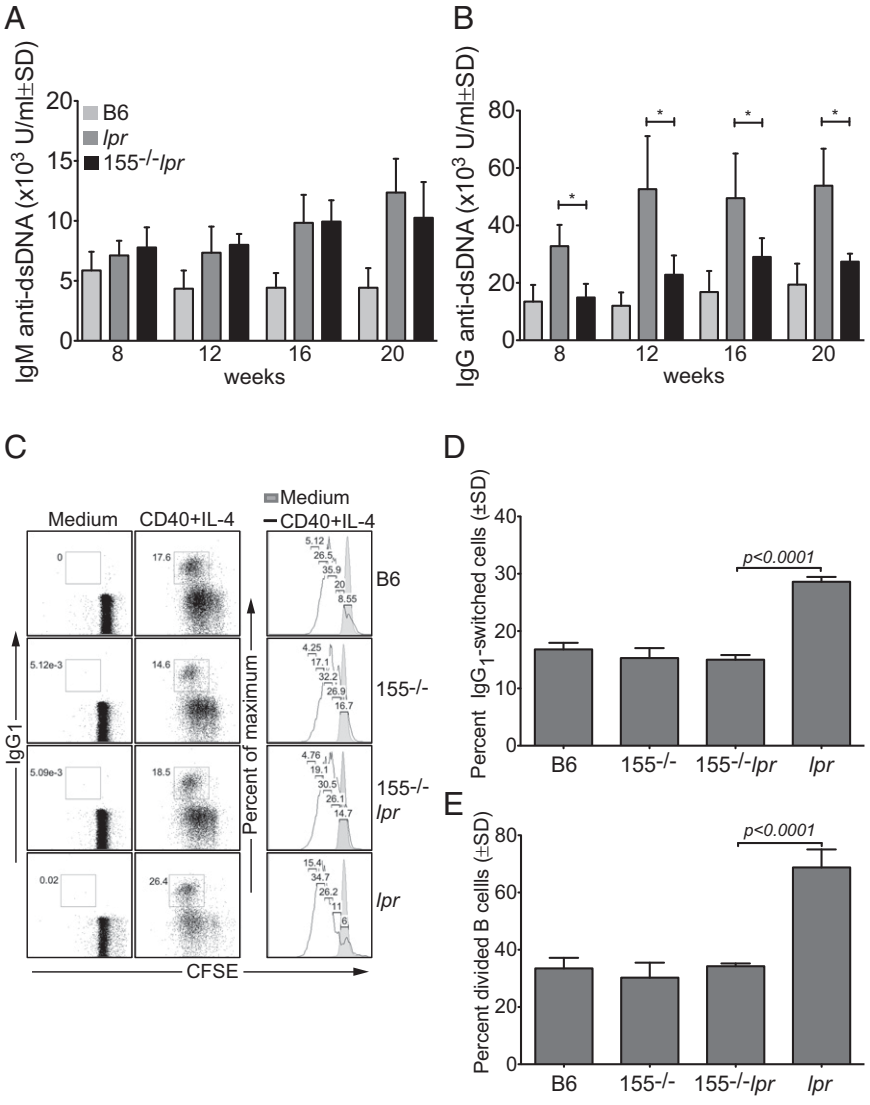

Fig. 3. Serum IgG anti-dsDNA autoantibodies are decreased in miR-155$^{-/-}$-*Fas*^{lpr} mice. (*A* and *B*) Serum IgM and IgG anti-dsDNA antibodies were measured by ELISA, and levels were expressed as arbitrary units; $*P \leq 0.02$. (*C*) Naïve spleen B cells were labeled with CFSE and induced to divide and class switch in vitro for 3 d with 2 μg/mL anti-CD40 Ab (clone HM40-3) and 25 ng/mL IL-4. Cell division was determined with FlowJo Proliferation Platform software. Dead cells were excluded by the DNA vital dye TO-PRO-3. (*D* and *E*) Compilation of results obtained in *C*. *P* values were determined by Student *t* test (GraphPad Software).

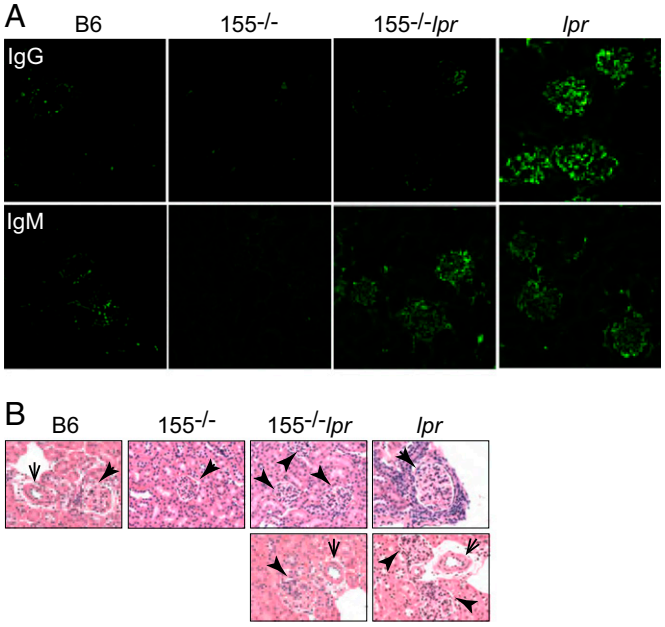

Fig. 4. MiR-155 deficiency alleviates renal pathologies in *fas*-deficient lupus-prone mice. Kidneys were obtained from 10- to 12-mo-old mice. (*A*) Confocal microscopy was done to determine IgG and IgM (green) deposition on kidney sections. (*B*) Kidney morphology was assessed by histology with H&E stain. Thick and thin arrows indicate glomeruli and vessels, respectively.

compared with the large amounts of IgG seen in Fas^{lpr} kidneys (Fig. 4*A*). The IgG signal intensity in B6 and miR-155$^{-/-}$ control kidneys was negligible (Fig. 4*A*). By contrast, IgM deposition remained similar in kidneys of Fas^{lpr} and miR-155$^{-/-}$-Fas^{lpr} mice, consistent with the fact they had comparable levels of serum IgM (Fig. 4*A*). Extensive IgG positivity was also observed in the medulla and vessels of Fas^{lpr} kidneys but not in the corresponding areas of miR-155$^{-/-}$-Fas^{lpr} kidneys (Fig. S4 *A* and *B*). Histopathologic analyses of kidneys from Fas^{lpr} mice showed enhanced mononuclear cell infiltration, disrupted architecture, and enlarged glomeruli (Fig. 4*B* and Fig. S5, thick and thin arrows indicate glomeruli and vessels, respectively). By contrast, the kidneys of age-matched miR-155$^{-/-}$-Fas^{lpr}, B6, and miR-155$^{-/-}$ mice showed little or no abnormalities in the overall architecture, negligible levels of mononuclear cell infiltration, and contained normal-size glomeruli, correlating with the absence of IgG staining. Lower serum IgG autoantibody levels were associated with improved renal clinical parameters in miR-155$^{-/-}$-Fas^{lpr} mice (Table S1). Urinalysis of the compound mutant mice, using Multistix strips, revealed only trace amounts of blood and an undetectable number of lymphocytes, similar to WT B6 and miR-155$^{-/-}$ mice. Although the level of urinary proteins in the miR-155$^{-/-}$-Fas^{lpr} mice was higher than that of WT B6 and miR-155$^{-/-}$ mice, it was fourfold lower than in Fas^{lpr} mice (53 ± 36 vs. 260 ± 89, $P = 0.0006$). Collectively, our results demonstrate that targeting miR-155 in the lupus-prone Fas^{lpr} mouse leads to decreased IgG deposition and renal damages.

MiR-155 Modulates SHIP-1 Expression and the Downstream ERK Kinase Pathway After BCR and FcγRIIB Coligation. Although our data suggest that miR-155 plays an essential role in regulating autoantibody responses in lupus-prone Fas^{lpr} mice, the mechanisms by which miR-155 exerts its regulatory functions are not readily apparent. It has been proposed that miR-155 regulates SHIP-1 expression in mammalian myeloid and malignant B cells (28–31). However, it is not known whether SHIP-1 regulation by miR-155 affects GC reactions or peripheral tolerance during a protective immune response or in an autoimmune environment, such as that in Fas^{lpr} mice. We previously showed that although miR-155 levels are negligible in resting B cells, stimulation induces a transient peak of miR-155 expression at 24 h (1). Because spleens from Fas^{lpr} mice contained B cells with an activated/GC phenotype, we asked whether miR-155 would be detected in these cells. As shown in Fig. 5*A*, resting and activated CD19$^+$ spleen B cells from Fas^{lpr} mice expressed miR-155. By contrast, miR-155 was only present in activated spleen B cells from B6 mice. MiR-155 was not detected in either miR-155$^{-/-}$ or miR-155$^{-/-}$-Fas^{lpr} B cells, as expected. Whereas treatment with intact goat IgG anti-IgM (BCR) had little effects on SHIP-1 levels in B6 B cells, miR-155–deficient B cells had a 2.4-fold increase in SHIP-1 levels after treatment, as measured by Western immunoblots (Fig. 5*B*). We observed little difference in SHIP-1 steady-state expression in unstimulated B6, miR-155$^{-/-}$, and miR-155$^{-/-}$-Fas^{lpr} spleen B cells, consistent with the fact that miR-155 is not expressed in resting normal B cells. SHIP-1 protein expression was lower in unstimulated Fas^{lpr} spleen B cells and was unaffected by our stimulation, perhaps because miR-155 was constitutively present in these cells. By contrast, SHIP-1 levels in miR-155$^{-/-}$-Fas^{lpr} spleen B cells increased after activation compared with Fas^{lpr}, but still lower than that of miR-155$^{-/-}$ B cells. Thus, miR-155 deficiency restores SHIP-1 expression levels in Fas^{lpr} spleen B cells, suggesting that in the *lpr* background, miR-155 is at least partially responsible for poor SHIP-1 expression in B cells. These results also suggest that upon activation, miR-155 is induced to maintain a SHIP-1 level that would prevent the prolongation of SHIP-1 inhibitory effects on B-cell activation. However, in Fas^{lpr} B cells, the persistent presence of miR-155 keeps SHIP-1 levels low, thus allowing these cells to be readily activated.

Next we asked whether ERK activation is affected by the dysregulated SHIP-1 expression in miR-155–deficient B cells. Indeed, after BCR and FcγRIIB coengagement, ERK phosphorylation was dampened in miR-155$^{-/-}$ and miR-155$^{-/-}$-Fas^{lpr} spleen B cells compared with B6 controls (Fig. 5*C*). Fas^{lpr} B cells displayed a higher level of ERK activation after engagement of the BCR and the FcγRIIB, corresponding to the lower level of SHIP-1 seen in these cells. In the absence of FcγRIIB coengagement [goat IgG (Fab')$_2$], hence no inhibitory signal, the ERK activation state remained similar in spleen B cells from mice of all genotypes (Fig. 5*D*). There was negligible ERK activation in all unstimulated cultures. Thus, our results implicate

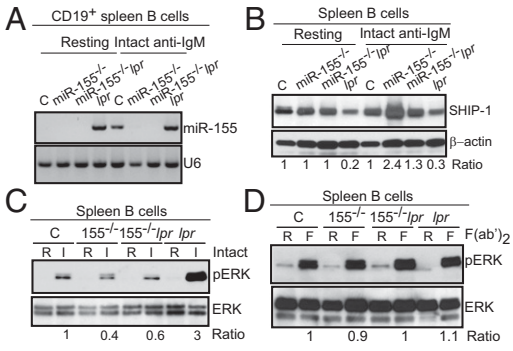

Fig. 5. MiR-155 modulates SHIP-1 expression and the downstream ERK kinase pathway after BCR and FcγRIIB coligation. (*A*) CD19$^+$ spleen B cells were left untouched or activated with intact IgG anti-IgM for 16 h. MiR-155 or U6 was probed from 2 μg of total RNA per sample. (*B*) CD19$^+$ spleen B cells were left untouched or activated with intact IgG anti-IgM for 24 h. Whole-cell lysates were probed with an anti-SHIP-1 antibody followed by anti-β-actin. Results are representative of three independent experiments with six mice per genotype. Ratio: total SHIP-1/β-actin determined by Bio-Rad Quantity One software. (*C* and *D*) Naïve spleen B cells were activated with intact IgG anti-IgM (*C*) or with F(ab')$_2$ anti-IgM (*D*) for 15 min. Whole-cell lysates were probed with anti-phospho-ERK, stripped, then reprobed with anti-total ERK. Ratio: pERK/total ERK determined by Bio-Rad Quantity One software. Results are representative of three independent experiments with six mice per genotype.

miR-155 in the suppression of SHIP-1 while promoting the activation of the ERK–kinase signaling pathway in both nonautoimmune and autoimmune mice. The elevated ERK activation status observed in *Fas*^{lpr} B cells likely results from reduced SHIP-1 expression levels in these cells. Our observations suggest a mechanism whereby miR-155 controls SHIP-1 levels to maintain a certain B-cell activation threshold after coaggregation of the BCR and FcγRIIB by immune complexes.

MiR-155 Controls B-Cell Proliferation Through SHIP-1. Because SHIP-1 controls cell proliferation after BCR and FcγRIIB coligation, we reasoned that the increased SHIP-1 expression and decreased ERK activation would lead to a lower proliferation rate of miR-155$^{-/-}$ and miR-155$^{-/-}$-*Fas*^{lpr} activated B cells, and that engagement of the BCR alone would have no effects. After BCR and FcγRIIB coengagement, cell proliferation was decreased in all cultures compared with activation through the BCR alone (Fig. 6 *A* and *B*). However, after coligation of the BCR and FcγRIIB, we observed a further 1.9-fold reduction in the frequency of divided cells in miR-155$^{-/-}$ B-cell cultures (14% ± 1%) compared with B6 (26% ± 1.2%, $^{*}P = 0.0003$, Fig. 6*B*). Likewise, there was a twofold decrease in the number of divided cells in miR-155$^{-/-}$-*Fas*^{lpr} (23% ± 3%) compared with *Fas*^{lpr} cultures (49% ± 4%, $^{**}P = 0.0022$). Furthermore, knock-down of *Inpp5d* (the gene encoding SHIP-1) in miR-155$^{-/-}$-*Fas*^{lpr} B cells partially restored ERK phosphorylation and cell proliferation (Fig. S6). The proliferation rate between B6 (26% ± 1.2%) and miR-155$^{-/-}$-*Fas*^{lpr} (23% ± 3%) cultures remained similar. There was no appreciable difference in the frequency of divided cells or cell death in all cultures in the absence of FcγRIIB coaggregation (Fig. 6 *A* and *B* and Fig. S6). After coligation of the BCR and FcγRIIB, miR-155$^{-/-}$ and miR-155$^{-/-}$-*Fas*^{lpr} cultures contained more dead cells compared with controls, as measured by the DNA vital dye TO-PRO-3 (Fig. S7). As expected, the percentage of cell death was highest in all cultures that did not receive stimuli (Fig. S7). Thus, miR-155 deficiency normalized *Fas*^{lpr} B-cell proliferation rate to that of B6. We propose that the reduction of autoreactive B cells in the miR-155$^{-/-}$-*Fas*^{lpr} mouse results in part from the recovery of SHIP-1 expression, leading to an attenuation of B-cell activation pathways induced by immune complexes.

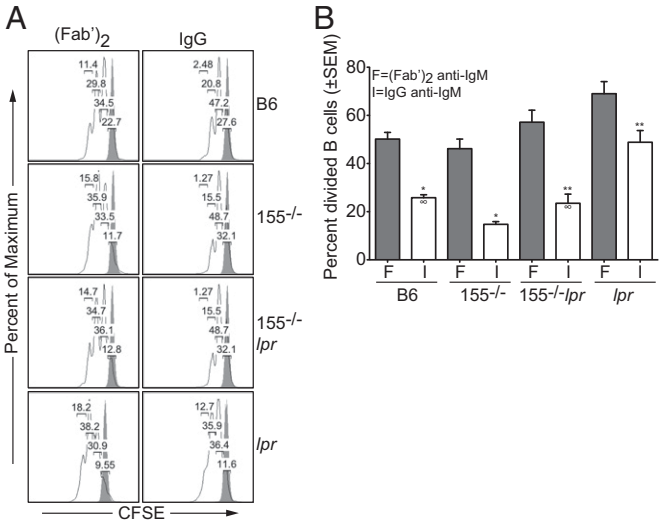

Fig. 6. MiR-155 controls B-cell proliferation through SHIP-1 after BCR and FcγRIIB coligation. (*A*) Naïve spleen B cells were labeled with CFSE and stimulated with either intact IgG or F(ab')$_2$ anti-IgM for 3 d. Cell division was determined using FlowJo Proliferation Platform software. Results are representative of four independent experiments with eight mice per genotype. (*B*) Same as in *A*. F, (Fab')$_2$ anti-IgM; I, intact IgG anti-IgM. $^{*}P = 0.0003$; $^{**}P = 0.0022$; $^{\infty}P = 0.6097$ determined by Student *t* test. Results are from four independent experiments with eight mice per genotype.

Discussion

In this study, we asked whether and how miR-155 regulates systemic autoimmunity. We find that ablation of miR-155 reduces autoantigen-induced GC reactions in spleens and pLNs of lupus-prone *fas*-deficient mice. There was a strong decrease in the level of serum IgG anti-dsDNA but not IgM anti-dsDNA autoantibodies. Correspondingly, miR-155$^{-/-}$-*Fas*^{lpr} mice show greatly reduced IgG but not IgM deposition in their kidneys, and renal pathologies were almost completely abrogated. Mechanistically, we show that miR-155 in part controls the expression of SHIP-1 in spleen B cells. Coaggregation of the BCR with FcγRIIB leads to an increase in SHIP-1 protein and impaired ERK activation in miR-155$^{-/-}$ B cells compared with B6 B cells. We find that naïve as well as activated *Fas*^{lpr} B cells are defective in SHIP-1 expression, whereas ERK activation is enhanced. MiR-155 deficiency in the *Fas*^{lpr} mouse restores SHIP-1 expression and mitigates ERK activation, cell proliferation, and the production of switched antibodies.

In the *lpr* autoimmune environment, miR-155 controls IgG but not IgM responses to chronic autoantigen exposure. Likewise, in germ line-deleted miR-155 mice or mice receiving miR-155$^{-/-}$ bone marrow, miR-155 does not affect IgM responses to haptenated proteins such as NP-CGG or NP-KLH (3). By contrast, germ line-deleted miR-155 mice infected with the live-attenuated form of the enteric pathogen *Salmonella typhimurium* or with the unhaptenated T-dependent antigen tetanus toxin fragment C protein have reduced serum IgM (2). Together, these observations suggest that in both systemic autoimmune and nonautoimmune environments, the nature and dose of the antigen, as well as the site and duration of exposure to the antigen, elicit distinct signals and mechanisms governing IgG vs. IgM responses, which are likely under the control of miR-155.

In human and mouse, switched autoantibodies to nuclear antigens are shown to be derived from both extrafollicular and GC reactions (15, 37–45). In response to exogenous antigens, miR-155 regulates both GC and non-GC reactions. Therefore, our results suggest that in the *Fas*^{lpr} mouse, targeting miR-155 likely affects both GC and extrafollicular responses, leading to the reduction of IgG autoantibodies, which are pathogenic.

Mice harboring B-cell-specific FcγRIIB or SHIP-1 deletion develop severe lupus-like disease characterized by the presence of high-titer serum antinuclear and antikidney autoantibodies, lymphadenopathy, splenomegaly, and renal pathologies (23–27). Thus, our results suggest that miR-155 in part modulates the expression level of SHIP-1 after coligation of the BCR and FcγRIIB by immune complexes. SHIP-1 in turn regulates the threshold of B-cell activation through the ERK signaling pathway. By targeting miR-155 in the *Fas*^{lpr} mouse, we could block the persistent activation of switched autoreactive B cells, thus alleviating lupus-like disease. Our results offer insights into how autoimmunity is regulated by miR-155 and suggest the possibility of targeting miR-155 to treat autoimmunity while preserving the protective immunity (46, 47).

Materials and Methods

Generation of Mutant Mice. To generate miR-155$^{-/-}$-*Fas*^{lpr} double-mutant mice, we crossed B6-*Fas*^{lpr} mice (Jackson Laboratory) with our *bic*/miR-155$^{-/-}$ mice (1). C57BL/6 were purchased from Jackson Laboratory. *bic*/miR-155$^{-/-}$ mice were maintained in house. All mice were bred and maintained in specific pathogen-free conditions. All mouse protocols were approved by the Beth Israel Deaconess Medical Center Institutional Animal Care and Use Committee.

ELISA. To determine IgG anti-dsDNA antibody, ELISA (Alpha Diagnostic) was performed using serum from 8-wk-old to 20-wk-old mice, according the manufacturer's recommendations.

Urinalysis. To determine kidney functions, urine was collected from aged mice. Multistix 10 SG strips and the CLINITEKStatus machine (Siemens) were used to determine the presence of blood, lymphocytes, and proteins in urine samples.

Histology, Immunohistochemistry, and Immunofluorescence. Four-micrometer tissue sections of kidneys were used. The following reagents were used: biotinylated PNA (Vector Laboratories); anti-streptavidin-HRP Envision+ kit (DAKO USA); goat anti-mouse IgG (SouthernBiotech); goat anti-mouse IgM $(Fab')_2$ fragments (Jackson ImmunoResearch Laboratories); and donkey anti-goat-Alexa-488 (1:200, Life Technologies). Images were acquired with a Zeiss 710 laser scanning confocal microscope and analyzed with Zen 2010 and ImageJ software. All images were ~400 μM.

In Vitro B-Cell Activation and Isotype Switch Assay. Magnetic-activated cell sorting (MACS)-purified (Miltenyi Biotec) $CD43^-$ or $CD19^+$ B cells were activated in vitro at a density of $1–3 \times 10^6$ cells/mL with 2 μg/mL of anti-CD40 clone HM40-3 (eBiosciences) plus 25 ng/mL of recombinant mouse IL-4 (R&D Systems), 10 μg/mL of goat $F(ab')_2$ anti-mouse IgM, or with 10 μg/mL of goat IgG (intact) anti-mouse IgM antibody (Jackson Immunoresearch).

Proliferation Assays and Analysis. MACS-purified $CD43^-$ B cells labeled with Carboxyfluorescein succinimidyl ester (CFSE) CFSE were activated with indicated stimuli as above for 3 or 4 d. Data were analyzed using the proliferation platform of FlowJo software (Tree Star).

Western Immunoblot Assays. Pellets were lysed with RIPA buffer containing protease inhibitors (Roche). The following antibodies were used: rabbit anti-SHIP-1 monoclonal antibody (catalog no. 2727), rabbit anti-phospho-p44/42 (pErk1/2) MAPK antibody, and rabbit anti-p44/42 (Erk1/2) MAPK antibody; all antibodies were purchased from Cell Signaling Technology. Anti-mouse β-actin was purchased from Sigma-Aldrich. For chemiluminescence detection, we used the Fujifilm LAS-4000 imaging system.

Northern Blot Assays. Northern blots were carried out using the Signosis high sensitive system per the manufacturer's suggestions (Signosis). Briefly, 2 μg of total RNA was separated through gel electrophoresis and transferred onto a membrane. Expression of miR-155 or U6 was detected with a biotin-labeled probe. For chemiluminescence detection, we used the Fujifilm LAS-4000 imaging system.

Statistical Analysis. *P* values were determined by applying Student's two-tailed *t* test for independent samples, assuming equal variances on all experimental data sets, using the online *t* test calculator from GraphPad Software.

ACKNOWLEDGMENTS. We thank Aliakbar Shahsafaei at the Brigham and Women Hospital pathology core for excellent histology, immunohistochemistry, and immunofluorescence work. This work was supported by National Institutes of Health Grants AI099012 (to T.-H.T.) and AI42269 (to G.C.T.).

1. Thai TH, et al. (2007) Regulation of the germinal center response by microRNA-155. *Science* 316(5824):604–608.
2. Rodriguez A, et al. (2007) Requirement of bic/microRNA-155 for normal immune function. *Science* 316(5824):608–611.
3. Vigorito E, et al. (2007) microRNA-155 regulates the generation of immunoglobulin class-switched plasma cells. *Immunity* 27(6):847–859.
4. Stagakis E, et al. (2011) Identification of novel microRNA signatures linked to human lupus disease activity and pathogenesis: miR-21 regulates aberrant T cell responses through regulation of PDCD4 expression. *Ann Rheum Dis* 70(8):1496–1506.
5. Hao Z, et al. (2008) Fas receptor expression in germinal-center B cells is essential for T and B lymphocyte homeostasis. *Immunity* 29(4):615–627.
6. Pritchard NR, et al. (2000) Autoimmune-prone mice share a promoter haplotype associated with reduced expression and function of the Fc receptor FcgammaRII. *Curr Biol* 10(4):227–230.
7. Jiang Y, et al. (1999) Genetically determined aberrant down-regulation of FcgammaRIIB1 in germinal center B cells associated with hyper-IgG and IgG autoantibodies in murine systemic lupus erythematosus. *Int Immunol* 11(10):1685–1691.
8. Jiang Y, et al. (2000) Polymorphisms in IgG Fc receptor IIB regulatory regions associated with autoimmune susceptibility. *Immunogenetics* 51(6):429–435.
9. Davis RS, Wang YH, Kubagawa H, Cooper MD (2001) Identification of a family of Fc receptor homologs with preferential B cell expression. *Proc Natl Acad Sci USA* 98(17):9772–9777.
10. Jackson TA, Haga CL, Ehrhardt GR, Davis RS, Cooper MD (2010) FcR-like 2 Inhibition of B cell receptor-mediated activation of B cells. *J Immunol* 185(12):7405–7412.
11. Kochi Y, et al. (2009) FCRL3, an autoimmune susceptibility gene, has inhibitory potential on B-cell receptor-mediated signaling. *J Immunol* 183(9):5502–5510.
12. Kochi Y, et al. (2005) A functional variant in FCRL3, encoding Fc receptor-like 3, is associated with rheumatoid arthritis and several autoimmunities. *Nat Genet* 37(5):478–485.
13. Ravetch JV, Bolland S (2001) IgG Fc receptors. *Annu Rev Immunol* 19:275–290.
14. Isnardi I, Bruhns P, Bismuth G, Fridman WH, Daëron M (2006) The SH2 domain-containing inositol 5-phosphatase SHIP1 is recruited to the intracytoplasmic domain of human FcgammaRIIB and is mandatory for negative regulation of B cell activation. *Immunol Lett* 104(1-2):156–165.
15. Tiller T, et al. (2010) Development of self-reactive germinal center B cells and plasma cells in autoimmune Fc gammaRIIB-deficient mice. *J Exp Med* 207(12):2767–2778.
16. Xiang Z, et al. (2007) FcgammaRIIb controls bone marrow plasma cell persistence and apoptosis. *Nat Immunol* 8(4):419–429.
17. Condé C, Gloire G, Piette J (2011) Enzymatic and non-enzymatic activities of SHIP-1 in signal transduction and cancer. *Biochem Pharmacol* 82(10):1320–1334.
18. Tamir I, Dal Porto JM, Cambier JC (2000) Cytoplasmic protein tyrosine phosphatases SHP-1 and SHP-2: Regulators of B cell signal transduction. *Curr Opin Immunol* 12(3):307–315.
19. Waterman PM, Cambier JC (2010) The conundrum of inhibitory signaling by ITAM-containing immunoreceptors: Potential molecular mechanisms. *FEBS Lett* 584(24): 4878–4882.
20. Vasudevan KM, Garraway LA (2010) AKT signaling in physiology and disease. *Curr Top Microbiol Immunol* 347:105–133.
21. Tamir I, et al. (2000) The RasGAP-binding protein p62dok is a mediator of inhibitory FcgammaRIIB signals in B cells. *Immunity* 12(3):347–358.
22. Mashima R, Hishida Y, Tezuka T, Yamanashi Y (2009) The roles of Dok family adapters in immunoreceptor signaling. *Immunol Rev* 232(1):273–285.
23. O'Neill SK, et al. (2011) Monophosphorylation of CD79a and CD79b ITAM motifs initiates a SHIP-1 phosphatase-mediated inhibitory signaling cascade required for B cell anergy. *Immunity* 35(5):746–756.
24. Helgason CD, et al. (2000) A dual role for Src homology 2 domain-containing inositol-5-phosphatase (SHIP) in immunity: Aberrant development and enhanced function of b lymphocytes in ship -/- mice. *J Exp Med* 191(5):781–794.
25. Helgason CD, et al. (1998) Targeted disruption of SHIP leads to hemopoietic perturbations, lung pathology, and a shortened life span. *Genes Dev* 12(11):1610–1620.
26. Bolland S, Ravetch JV (2000) Spontaneous autoimmune disease in Fc(gamma)RIIB-deficient mice results from strain-specific epistasis. *Immunity* 13(2):277–285.
27. Liu Q, et al. (1998) The inositol polyphosphate 5-phosphatase ship is a crucial negative regulator of B cell antigen receptor signaling. *J Exp Med* 188(7):1333–1342.
28. Cremer TJ, et al. (2009) MiR-155 induction by *F. novicida* but not the virulent *F. tularensis* results in SHIP down-regulation and enhanced pro-inflammatory cytokine response. *PLoS One* 4(12):e8508.
29. Pedersen IM, et al. (2009) Onco-miR-155 targets SHIP1 to promote TNFalpha-dependent growth of B cell lymphomas. *EMBO Mol Med* 1(5):288–295.
30. Costinean S, et al. (2009) Src homology 2 domain-containing inositol-5-phosphatase and CCAAT enhancer-binding protein beta are targeted by miR-155 in B cells of Emicro-MiR-155 transgenic mice. *Blood* 114(7):1374–1382.
31. O'Connell RM, Chaudhuri AA, Rao DS, Baltimore D (2009) Inositol phosphatase SHIP1 is a primary target of miR-155. *Proc Natl Acad Sci USA* 106(17):7113–7118.
32. Cohen PL, Eisenberg RA (1991) Lpr and gld: Single gene models of systemic autoimmunity and lymphoproliferative disease. *Annu Rev Immunol* 9:243–269.
33. Fortner KA, Lees RK, MacDonald HR, Budd RC (2011) Fas (CD95/APO-1) limits the expansion of T lymphocytes in an environment of limited T-cell antigen receptor/MHC contacts. *Int Immunol* 23(2):75–88.
34. Maldonado MA, et al. (1999) The role of environmental antigens in the spontaneous development of autoimmunity in MRL-lpr mice. *J Immunol* 162(11):6322–6330.
35. Satoh M, et al. (2007) Clinical implication of autoantibodies in patients with systemic rheumatic diseases. *Expert Rev Clin Immunol* 3(5):721–738.
36. Cohen-Solal J, Diamond B (2011) Lessons from an anti-DNA autoantibody. *Mol Immunol* 48(11):1328–1331.
37. William J, Euler C, Christensen S, Shlomchik MJ (2002) Evolution of autoantibody responses via somatic hypermutation outside of germinal centers. *Science* 297(5589):2066–2070.
38. William J, Euler C, Shlomchik MJ (2005) Short-lived plasmablasts dominate the early spontaneous rheumatoid factor response: Differentiation pathways, hypermutating cell types, and affinity maturation outside the germinal center. *J Immunol* 174(11):6879–6887.
39. William J, Euler C, Leadbetter E, Marshak-Rothstein A, Shlomchik MJ (2005) Visualizing the onset and evolution of an autoantibody response in systemic autoimmunity. *J Immunol* 174(11):6872–6878.
40. Shlomchik M, et al. (1990) Anti-DNA antibodies from autoimmune mice arise by clonal expansion and somatic mutation. *J Exp Med* 171(1):265–292.
41. Shlomchik MJ, Marshak-Rothstein A, Wolfowicz CB, Rothstein TL, Weigert MG (1987) The role of clonal selection and somatic mutation in autoimmunity. *Nature* 328(6133):805–811.
42. van Es JH, et al. (1991) Somatic mutations in the variable regions of a human IgG anti-double-stranded DNA autoantibody suggest a role for antigen in the induction of systemic lupus erythematosus. *J Exp Med* 173(2):461–470.
43. Winkler TH, Fehr H, Kalden JR (1992) Analysis of immunoglobulin variable region genes from human IgG anti-DNA hybridomas. *Eur J Immunol* 22(7):1719–1728.
44. Wellmann U, et al. (2005) The evolution of human anti-double-stranded DNA autoantibodies. *Proc Natl Acad Sci USA* 102(26):9258–9263.
45. Mietzner B, et al. (2008) Autoreactive IgG memory antibodies in patients with systemic lupus erythematosus arise from nonreactive and polyreactive precursors. *Proc Natl Acad Sci USA* 105(28):9727–9732.
46. Racine R, et al. (2011) IgM production by bone marrow plasmablasts contributes to long-term protection against intracellular bacterial infection. *J Immunol* 186(2):1011–1021.
47. Foote JB, Mahmoud TI, Vale AM, Kearney JF (2012) Long-term maintenance of polysaccharide-specific antibodies by IgM-secreting cells. *J Immunol* 188(1):57–67.